Identification of ebselen as a potent inhibitor of insulin degrading enzyme by a drug repurposing screening

Florence Leroux, Damien Bosc, Terence Beghyn, Paul Hermant, Sandrine Warenghem, Valérie Landry, Virginie Pottiez, Valentin Guillaume, Julie Charton, Adrien Herledan, et al.

Identification of ebselen as a potent inhibitor of Insulin Degrading Enzyme by a drug repurposing screening

Leroux, Florence;[1] Bosc, Damien;[1] Beghyn, Terence;[2] Hermant, Paul;[1] Warenghem, Sandrine;[1] Landry, Valérie;[1] Pottiez, Virginie;[1] Guillaume, Valentin;[1] Charton, Julie;[1-5] Herledan, Adrien;[1] Urata, Sarah;[3] Liang, Wenguang;[4] Sheng, Li;[3] Tang, Wei-Jen;[4] Deprez, Benoit;[1-5] Deprez-Poulain, Rebecca[1,5-6*]

1. Univ. Lille, Inserm, Institut Pasteur de Lille, U1177 - Drugs and Molecules for Living Systems, F-59000 Lille, France;
2. APTEEUS, F-59000 Lille France;
3. Department of Medicine, University of California at San Diego, CA 92093 La Jolla, The United States.
4. Ben-May Institute for Cancer Research, the University of Chicago, IL 60637 Chicago, The United States.
5. European Genomic Institute for Diabetes, EGID, University of Lille, F-59000, France.
6. Institut Universitaire de France, F- 75231, Paris, France.

Keywords: enzymes • screening • inhibitors • ebselen • drug repurposing

* To whom correspondence should be addressed. R.D-P.: phone, (+33) (0)320 964 948 ; E-mail, rebecca.deprez@univ-lille.fr ; http://www.deprezlab.fr

Abstract :

Insulin-degrading enzyme, IDE, is a metalloprotease implicated in the metabolism of key peptides such as insulin, glucagon, β-amyloid peptide. Recent studies have pointed out its broader role in the cell physiology. In order to identify new drug-like inhibitors of IDE with optimal pharmacokinetic properties to probe its multiple roles, we ran a high-throughput drug repurposing screening. Ebselen, cefmetazole and rabeprazole were identified as reversible inhibitors of IDE. Ebselen is the most potent inhibitor ($IC_{50\ (insulin)}$ = 14 nM). The molecular mode of action of ebselen was investigated by biophysical methods. We show that ebselen induces the disorder of the IDE catalytic cleft, which significantly differs from the previously reported IDE inhibitors. IDE inhibition by ebselen can explain some of its reported activities in metabolism as well as in neuroprotection.

Abbreviations used

ADMA, asymmetrical dimethylarginine; DDAH, dimethylarginine dimethylaminohydrolase; DMSO, dimethylsulfoxide; EDTA, Ethylenediaminetetraacetic acid; IDE, Insulin-degrading enzyme; IDE-CF, cysteine-free IDE; GNAT, Gcn5-related N-acetyltransferase; HDAC, histone desaceylase; NDM-1, New Delhi metallo-β-lactamase; nitric oxide synthase, NOS; PBP, penicillin-binding protein; PBS, phosphate buffered saline; rt, room temperature;

1. Introduction

Insulin-Degrading Enzyme (IDE) is known for decades, yet its function remain poorly understood [1,2]. It is a ubiquitous, 110 kDa protease found in both intra- and extra-cellular compartments. IDE is a proteolytic enzyme involved in the degradation of many substrates [3]. In particular, it is the main enzyme responsible for the intracellular hydrolysis of insulin [4]. Glucagon [5] and amylin [6], other peptidic hormones secreted by the pancreas, are also substrates of IDE. Interestingly, along with insulin, these hormones regulate the metabolism of glucose and other energetic substrates like fatty acids. IDE was also proposed as one the enzymes involved in the catabolism of Aβ [7,8]. The involvement of IDE in the degradation of all these substrates suggests a potential role of IDE in processes modulated by these proteins. Interestingly, many substrates of IDE share a propensity to be amyloidogenic peptides [9].

IDE has an atypical structure that was solved in 2006 [10]. The displacement of IDE-N and IDE-C likely mediates the open-closed conformational switch required for the entrance of diverse substrates and the exit of products. Crystal structures of human IDE (hIDE) have revealed an IDE dimer with the fully closed catalytic chamber, though other experiments revealed that the open states are preferred in solution and allow the entry of large substrates (e.g. Aβ, or insulin) in the chamber. An unexpected displacement (swinging-door) of a subdomain that creates an 18Å opening to the chamber, which permits the entry of short peptides, has been postulated [11]. Recently, cryoEM structures of IDE open states and insulin-bound states revealed the mechanism by which amyloidogenic peptides, like insulin, are captured and hydrolyzed by IDE [12].

IDE has emerged as an atypical protein that is involved in many pathways [13].It has been shown to behave as a dead-end chaperone for aggregating peptides [14] ant to interact with the proteasome-ubiquitin system [15]. IDE has thus been shown to be involved in many

processes at the cellular level, but the phenotype of KO animals is very mild. Importantly, IDE's sequence is strikingly conserved amongst distantly related species, suggesting critical functions, Although these properties of IDE have raised the interest of biologists since many years without revealing its exact role, only a few teams have looked for inhibitors with probe-like properties, as a result only a couple of inhibitors that can be used *in vivo* are available.

First, Leissring *et al* disclosed a peptidomimetic inhibitor **Ii1** [16] (Fig. 1). Due to low permeability, this inhibitor was not tested in cellular assays. Our team has developed a series of carboxylic acids and ester pro-drugs like **BDM43079** and **BDM43124** respectively, that bind both a permanent exosite and the discontinuous, conformational catalytic site [17-18] (Fig. 1). Maianti *et al* disclosed **6bK** a macrocyclic peptide, binding at distance from the catalytic site, in the primary exosite pocket [19] (Fig. 1). Eli Lilly discovered the dual site inhibitor **NTE-1**, not interacting with the catalytic site, by a fragment-based strategy [20] (Fig. 1). Our team discovered drug-like compound **BDM44768** from an *in situ* click chemistry strategy [21] (Fig. 1). Surprisingly, **BDM44768**, **NTE-1** and **6bK** displayed different effects on glucose tolerance *in vivo*, underlying the complex role of IDE.

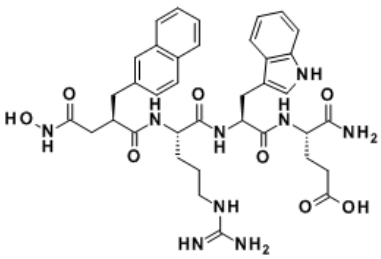

Ii1
(Ki = 1.7 nM)
Catalytic site

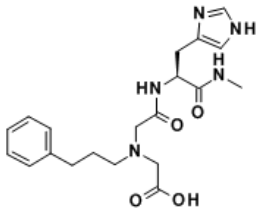

BDM44629
(IC_{50} = 100nM)
Exosite and Catalytic site

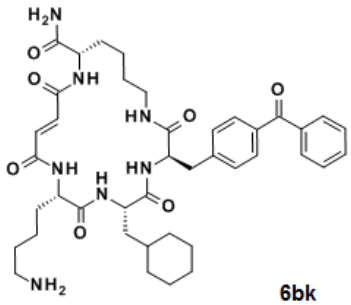

6bk
(IC_{50} = 50 nM)
Exosite

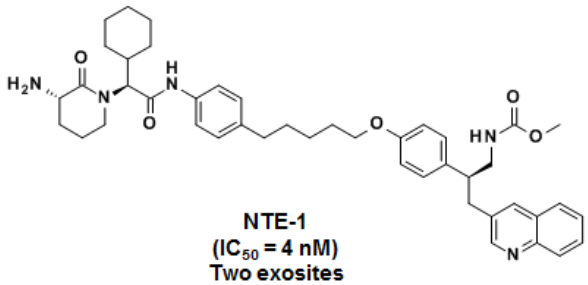

NTE-1
(IC_{50} = 4 nM)
Two exosites

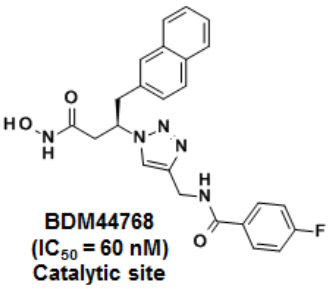

BDM44768
(IC_{50} = 60 nM)
Catalytic site

Fig. 1: Inhibitors of *h*IDE.

2. Results and Discussion

2.1. Screening of a 1120-member library.

With the aim of discovering new chemical probes having desired drug-like properties, to explore the complex role of hIDE, we screened at 30 µM a library of 1120 compounds that have reported clinical data (Fig. 2). The average Z′ factor value for assays is 0.61 and the percentage of inhibition of reference inhibitor EDTA 71% (Supporting information Table S1 and Fig. S1). Out of these compounds, 12 molecules displayed a percentage of inhibition above threshold (30%) at the screening concentration (Fig. 2). Dose-response curves were performed and 5 compounds (**1-5**) were confirmed (0.44% hit rate), with IC_{50}s ranging from 42 nM to 100 µM: rolitetracycline, myricetine, ebselen, cefmetazole and rabeprazole which display unique structural motifs and activities (Fig. 3 and Table 1). This hit rate is comparable to those published with other drug libraries (Prestwick, LOPAC…) screened on isolated targets (Supporting information Table S2).

Table 1: Inhibitory potencies of confirmed positives.

Cpd #	Name	IC_{50} (µM)[a]
1	rolitetracycline	100
2	myricetine	100
3	cefmetazole	7
4	rabeprazole	11
5	ebselen	0.042

[a] ATTO 655- Cys-Lys-Leu-Val-Phe-Phe-Ala-Glu-Asp-Trp substrate

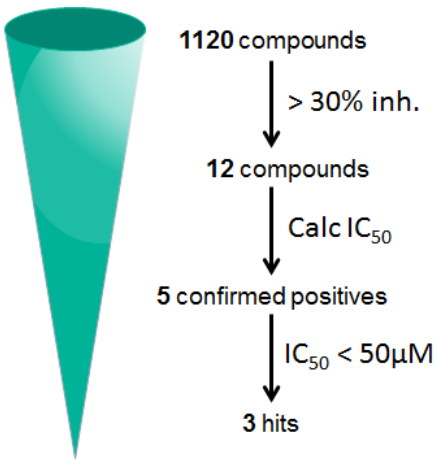

Fig. 2: Screening cascade.

Out of these compounds we selected cefmetazole (**3**), rabeprazole (**4**) and ebselen (**5**) for further investigation of mode of action and/or binding.

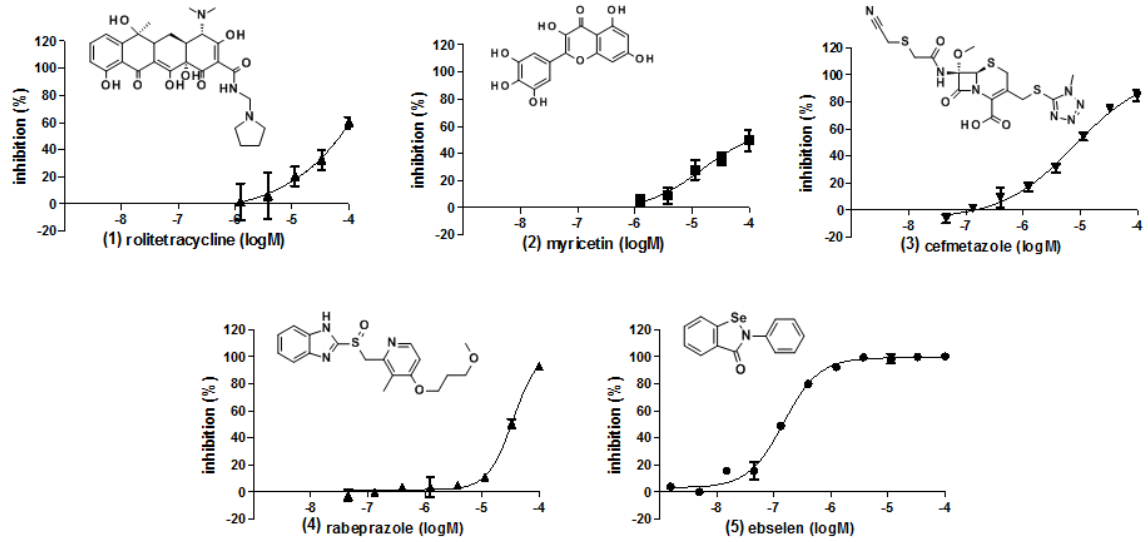

Fig. 3: Structures and DRCs of confirmed positives **1-5**.

2.2. *Cefmetazole **3***

2.2.1. *Reported activities.*

Cefmetazole **3** (IC_{50} = 7 µM) is a cephalosporin that inhibits irreversibly bacterial penicillin-binding proteins (PBP), the transpeptidases implicated in the peptidoglycan synthesis. Its mechanism is driven by the electrophilicity of the lactam function that forms an adduct with the catalytic serine in PBPs. It has been shown that cefmetazole behaves as a *pan* autophagy inhibitor suggesting the existence of eukaryotic targets [22]. It also inhibits the intracellular accumulation of α1-antitrypsin in a phenotypic screening in *C.elegans*. [23].

2.2.2. *Reversibility of inhibition of **3**.*

As cefmetazole **(3)** can react with nucleophile centers because its electrophilic behavior, we evaluated the reversibility of the binding of **3** to IDE (Fig. 4A). Cefmetazole at

50 µM inhibits hIDE (68% inhibition, green bar) while 0.5 µM of cefmetazole is inactive (cyan bar). Recovery of hIDE activity after large dilution (magenta bar) shows that cefmetazole **(3)** is a reversible inhibitor of hIDE (Fig. 4A), like **BDM44768** (Fig. 4C) while N-ethylmaleimide (**NEM**, Fig. 4D) is an irreversible inhibitor.

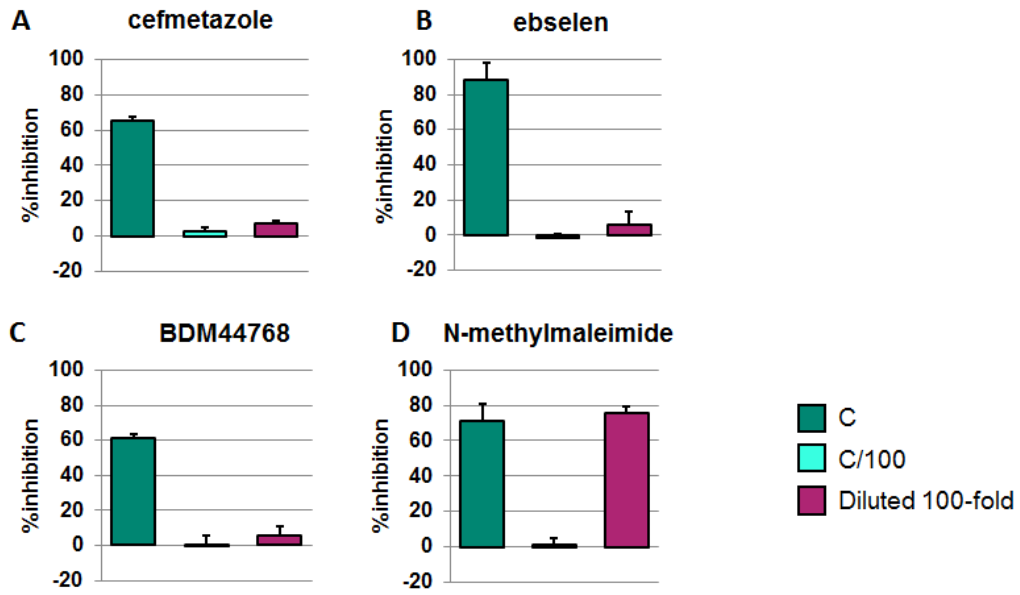

Fig. 4: Assessment of irreversible/reversible mechanism of inhibition.

Compounds identified in screening: cefmetazole **3** (A) and ebselen **5** (B) were pre-incubated 30 minutes at room temperature with hIDE before adding substrate (5µM), at final concentrations C (green bar) and 0.01C (cyan bar) respectively. Pre-incubate at C was diluted 100-fold (magenta bar) before adding the substrate. Percent of inhibition are mean of 4 experiments. **BDM44768** (C) a reversible inhibitor of hIDE and N-ethylmaleimide **NEM** (D) an irreversible inhibitor are used as controls. Recovery of hIDE activity minutes after large dilution (magenta bars) for cefmetazole **3** (A) and ebselen **5** (C) show that these compounds are reversible inhibitors of IDE.

*2.2.3. Binding of **3**.*

We docked **3** within hIDE (Fig. 6). In our model, cefmetazole **3** makes contacts with both N-term and C-term domains of hIDE. It interacts with the catalytic $Zinc^{2+}$ ion via its carboxylate group (Fig. 5). The lactam function makes a hydrogen bond with Gln111. The N-acetylated side chain of the cephalosporin is engaged in three interactions: an hydrogen bond

between the sulfur and the hydroxyle side-chain of Ser_{128}, interaction of NH with Arg_{824} and Asp_{182} via a hydrogen bond network with water molecules, and a hydrogen bond between the nitrile group and the backbone NH Ser_{138} (Fig. 5). In the model, no nucleophilic amino-acid could be seen in the vicinity of the lactam function. This binding mode is consistent with the reversible inhibition. Cefmetazole is the only cephalosporin displaying the nitrile side function, explaining why no other cephalosporin in the set was found to inhibit hIDE.

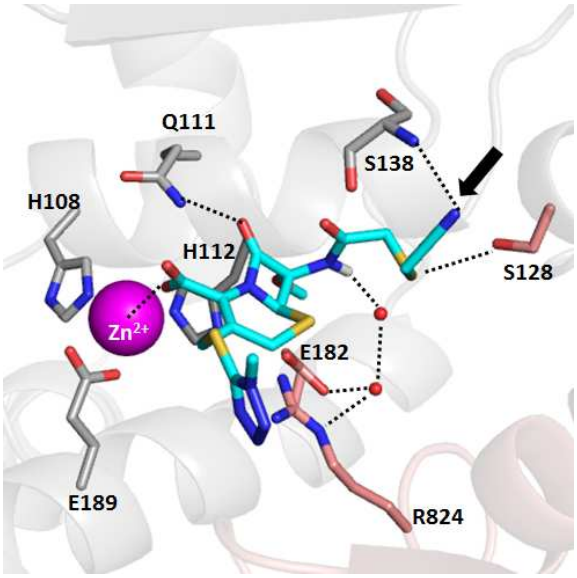

Fig. 5: Binding mode of cefmetazole in IDE.

Docked in PDB 4NXO. Oxygens, Nitrogens and Sulfurs are in red, blue and orange respectively, Carbons are in in gray (N-term) or light pink (C-term) for catalytic site amino-acids and in cyan for compounds. Polar hydrogens of cefmetazole are in white. Zinc ion is represented as a magenta sphere. Polar contacts and interactions are represented as black dashed lines. Nitrile function is pointed by black arrow.

*2.3. Rabeprazole **4**.*

2.3.1. Reported activities.

Rabeprazole (IC_{50} = 11 µM) is a prodrug that inhibits covalently the proton H^+/K^+ ATPase pump after activation into a sulphenamide. As such, it is used to inhibit gastric acid secretion and thus treat ulcers and gastro-intestinal reflux. All approved proton-pump inhibitors (PPI) contain the 2-pyridylmethylsulfinylbenzimidazole scaffold. Rabeprazole has

also been reported, along with other PPI, as an inhibitor (IC_{50} = 53 µM) of dimethylarginine dimethylaminohydrolase (DDAH), an enzyme that metabolizes asymmetrical dimethylarginine (ADMA), an endogenous and competitive inhibitor of nitric oxide (NO) synthase (NOS) [24]. More recently, rabeprazole was disclosed to be an inhibitor of endo-beta-N-acetylglucosaminidase (ENGase) (IC_{50} = 4 µM) [25]. We show here that IDE is another point of interaction of rabeprazole with the proteome

2.3.2. Mode of inhibition, binding and preliminary SAR.

In our model, rabeprazole interacts with both N-term and C-term domains of hIDE. Both the N-3 of benzimidazole ring and the oxygen of the sulfoxide function of rabeprazole interact with the Zn^{2+} ion (Fig. 6). The N-1 of the benzimidazole ring makes a hydrogen bond with Asn139. Pyridine and Arg824 are engaged in a cation-π interaction. Of note, 3-methoxypropyl-oxy side-chain makes a hydrogen-bond with Ser128 and a hydrogen-π interaction with Phe115 (Fig. 6).

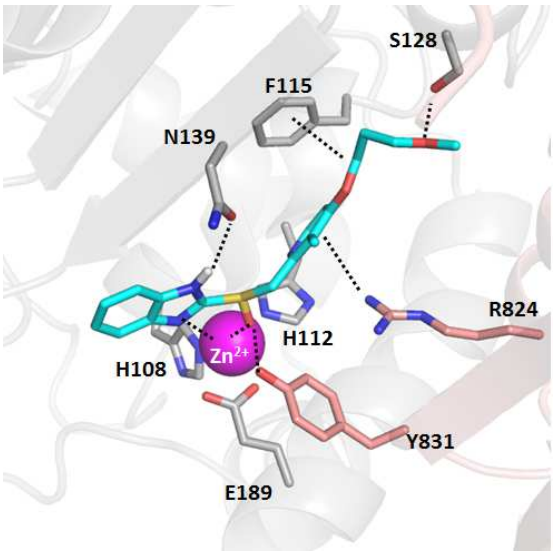

Fig. 6: Binding mode of rabeprazole in IDE.

Docked in PDB 4NXO. Oxygens, Nitrogens and Sulfurs are in red, blue and orange respectively, Carbons are in gray (N-term) or light pink (C-term) for catalytic site amino-acids and in cyan for rabeprazole. Polar hydrogens of rabeprazole are in white. Zinc ion is represented as a magenta sphere. Polar contacts and interactions of rabeprazole with hIDE are represented as black dashed blacklines.

Interestingly, several other PPI were in the screening library. Comparison of activities revealed that rabeprazole was by far the most potent analogue. Absence of substituent on the benzimidazole along with a long propylether chain in R2 may account for the better activity of rabeprazole in comparison with other pharmacological class members (Table 2). Indeed, docking studies show that the oxygen of the sulfoxide moiety of rabeprazole interacts with the Zn^{2+} ion while the long propyl ether chain is engaged in a unique interaction with Ser_{128} and Phe_{115}.

Table 2: Compared activities of proton-pump inhibitors on hIDE

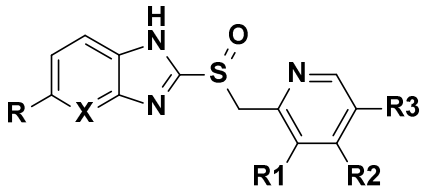

Compound	IC_{50} (µM) (%inb @100µM)	X	R	R1	R2	R3
omeprazole	_ (41)	C	CH_3O-	CH_3-	CH_3O-	CH_3-
lansoprazole	_ (38)	C	H-	CH_3-	CF_3-CH_2O-	H-
pantoprazole	_ (0)	C	CHF_2O-	CH_3O-	CH_3O-	H-
tenatoprazole	_ (35)	N	CH_3O-	CH_3-	CH_3O-	CH_3-
rabeprazole	11 (98)	C	H-	CH_3-	CH_3O-$(CH_2)_3$-O-	H-

2.4. Ebselen ***5****.*

2.4.1. Reported activities.

Ebselen, the most potent inhibitor (IC_{50} = 42 nM), is a seleno-organic compound that is known to make covalent bonds with cysteines [26]. Multiple bioactivities have reported in the literature for ebselen (Supporting information Table S3 and S4). Historically, ebselen was described as a gluthation peroxidase mimic. Zhao *et al*. suggested then that the antioxidant and anti-inflammatory actions of ebselen were due to its activity as a substrate of thioredoxine reductase [27]. Ebselen also reacts with hydroperoxides in membranes to protect cells from free radical damage [28-29]. Along with these activities, ebselen inhibits directly several enzymes involved in inflammation processes like NO synthases, NADPH oxidase, protein

kinase C and H^+/K^+-ATPase, lipooxygenases [29,30] by reacting with cysteines to form selenosulfide complexes (Supplementary Table S2). Due to these properties, it has been evaluated in the protection of the brain after ischemia and stroke both in animal models [31] and in humans [32]. In the latter trial, ebselen, at 10 mg kg^{-1}, significantly reduced the volume of infarction in brain. Ebselen was recently proposed as an anticancer agent on the basis of histone desacetylases (HDAC) inhibition or methionine aminopeptidases (MetAP), a protease involved in angiogenesis [33,34]. Finally, a recent report describes the inhibition of glutamate dehydrogenase (GDH) by ebselen [35].

Ebselen has also been tested against infectious diseases (Supporting information Table S4). Most recent examples include inhibition of New Delhi metallo-β-lactamase (NDM-1) [36], activity against resistant staphylococci [37] or binding to antigen 85C from *Mycobacterium tuberculosis* [38]. Ebselen is also an inhibitor of *Tb*HK1 from the parasite *Trypanosoma brucei* [39]. Finally, several antiviral activities have been reported recently. Ebselen is an inhibitor of HIV-1 capsid dimerization [40] and of Hepatitis C Helicase NS3 binding to nucleic acids [41]. Importantly, in most cases, ebselen was shown to be a covalent, irreversible ligand (inhibitor) of these proteins. Recently, ebselen was found by screening to be an inhibitor of bacterial and human inosine 5'-monophosphate dehydrogenase [42].

2.4.2. Mode of inhibition.

Ebselen is a thiol reactive compound. IDE contains 13 cysteines (Fig. 7), some of which have been proven important for catalytic activity [43]. We used the cysteine-free IDE (IDE-CF), that is still catalytically active, to probe the implication of the cysteines in the inhibition mode of ebselen [44]. In these conditions, ebselen is not active (2% inhibition at 100µM) (Table 3).

Table 3: Activity of ebselen on hIDEwt and hIDE-CF.

	hIDEwt	hIDE-CF
	IC_{50} (µM)	
ebselen	0.042	> 100
	0.014[a]	_[b]

BDM44768	0.30 0.056 [a]	0.33 – [b]
cefmetazole	7.0	(70%)[c]

[a] with insulin as substrate; [b] not determined; [c] percent of inhibition at 30µM.

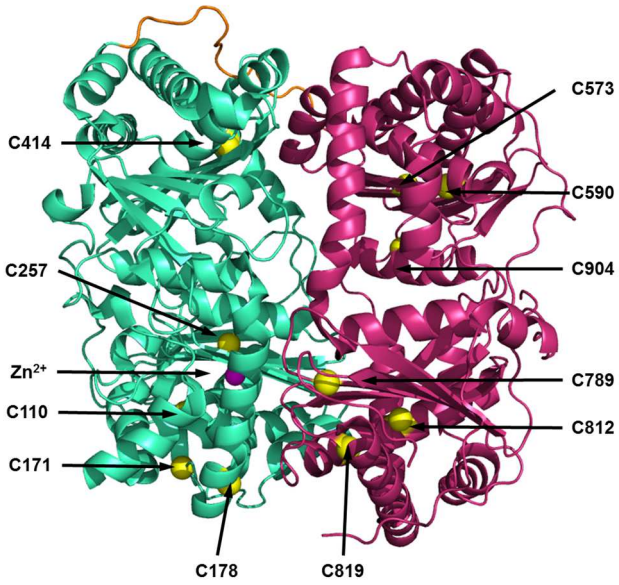

Fig. 7: Cysteines in *h*IDE.

From PDB 4NXO. N-terminal part in cyan, C-term part in warm pink, hinge in orange, Zinc ion represented as magenta sphere, C-α of 11 cysteines represented as yellow spheres.

Many thiol-reactive agents act through irreversible binding but some act as reversible inhibitors. Ebselen at 1.25 µM inhibits *h*IDE (88% inhibition, green bar, Fig. 4B) while 0.0125µM of ebselen is inactive (cyan bar). Ebselen was pre-incubated at 1.25 µM for 30 minutes at room temperature with *h*IDE. Pre-incubate was diluted 100-fold (magenta bar) before adding the substrate. Recovery of *h*IDE activity after large dilution (magenta bar) shows that ebselen is a reversible inhibitor. As we showed that its activity is dependent on cysteines, this suggests that ebselen could be a reversible covalent inhibitor of IDE. Recently, IDE was identified (among 461 other proteins) as a putative binding protein of ebselen in Hela cells, using a biotinylated probe [45].

2.4.3. Binding mode of ebselen.

Attempts to dock ebselen within hIDE did not allow to find relevant pockets containing cysteines to rationalize previous results. Thus, we characterized the interaction of IDE with ebselen experimentally. Human IDE has 10-20 nM affinity to each other to form a dimer [1]. We used the size exclusion chromatography (SEC), Superdex 200 10/300 GL to examine if ebselen affected IDE dimerization. As expected, 110 kDa IDE migrates mostly as dimer (Fig. 8). The addition of ebselen shifted IDE from mostly a dimer into a mixture of dimer and monomer (Fig. 8). The monomeric IDE is shown to be less active than the dimeric IDE [2, 3]. This suggests that a part of inhibitory effect by ebselen could be mediated by disrupting IDE dimerization.

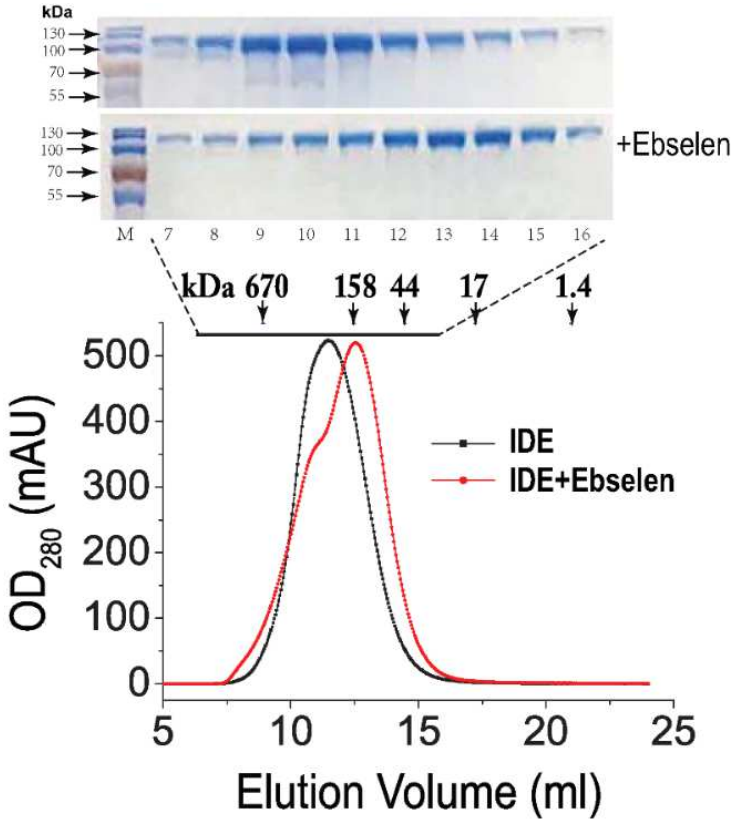

Figure 8 The effect of ebselen on the profile of IDE on size exclusion column. The top insert is the Coomassie stained 9% SDS-PAGE of peak fractions. M=marker.

Hydrogen/deuterium exchange mass spectrometry (HDX-MS) has been shown to effectively map the binding regions of two potent IDE inhibitors as well as depict the substrate-induced conformational changes of IDE [4]. We thus performed HDX-MS to probe the effect of ebselen on IDE (Fig. 9, Supporting information Fig. S3 and S4). While overall

differences of HD exchange of IDE were subtle when ebselen is present, such change provides insights into the action of ebselen. IDE dimer structure in conjunction with biochemical studies have shown that the C-terminal region of IDE plays a key role in IDE dimerization [2, 3, 5]. Consistent with this, we found that the C- terminal residues of IDE, 981-994 have enhanced HD exchange in the presence of ebselen. This corroborates with our gel-filtration data that ebselen promotes the dissociation of IDE dimer. The effect of ebselen to disrupt IDE dimerization could explain our failure to co-crystallize IDE with ebselen because all current hIDE crystallization conditions are for IDE dimer.

HDX-MS also provides additional information how ebselen affects IDE activity. We observed that residues 824-830 had significant enhanced HD exchange in the presence with ebselen. This region is part of the substrate binding cleft of IDE and the binding of substrates, e.g., insulin and amyloid [4]. Interestingly, two potent inhibitors of IDE, **6bK** and **BDM44768** significantly reduced the HD exchange of this region [4]. We also found that ebselen slightly reduced the HD exchange in residues 181-198, the region for the zinc binding catalytic cleft; such reduction was also observed when **6bk** and **BDM44768** were present [4]. Interestingly, close to both these regions stand cysteine residues (C178, C812 and C819). Together, the finding confirms that ebselen disrupts IDE dimerization and shows that it induces the disorder of the IDE catalytic cleft, which significantly differs from the previously reported IDE inhibitors, **BDM44768** and **6bK**.

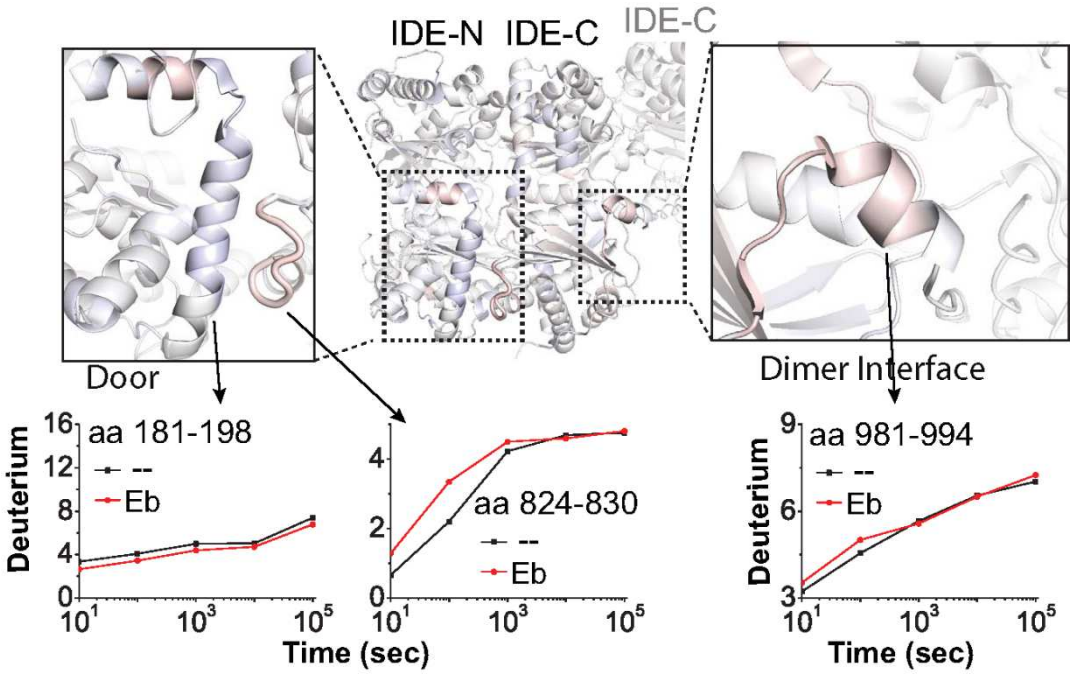

Figure 9 Changes in H/D exchange of IDE induced by ebselen.
The changes in H/D are mapped onto IDE structure and the progress curve of regions with significant changes are shown.

2.4.4. Target engagement in cells.

IDE is an enzyme that is both secreted and cytosolic [46]. We thus evaluated the ability of ebselen to bind IDE in insulin sensitive cells (HepG2) using the cellular thermal-shift assay (CETSA) technique [47] (Table 4). A quantification of the compounds in CETSA samples allowed to measure the cell/medium ratio of the compounds. These results show that ebselen and BDM44768 do penetrate cells to the same extend of 10%. Ebselen and **BDM44768** bind IDE in cells as shown by the shifts in the aggregation temperature in the presence of the compound. However the lower value for ebselen could reflect the titration of this compound by thiols within cells.

Table 4: Aggregation temperatures of hIDE in the presence of inhibitors and permeation.

Compound	T Agg (°C)	Delta Agg (°C)	Cell/medium ratio
BDM44768	54.4 ± 0.5	6.4 ± 0.5	0.11 ±0.02
ebselen	49.2 ± 0.2	1.3 ± 0.3	0.10±0.01

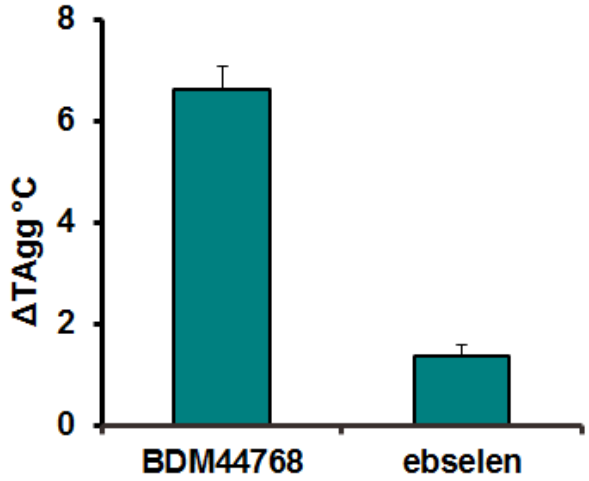

Figure 10 Cell target engagement of hIDE by compounds.

Aggregation temperature shifts of hIDE in the presence of inhibitors **BDM44768** and ebselen **5** normalized to DMSO.

3. Conclusion.

We have successfully identified, though a drug-repurposing high-throughput screen, 3 potent inhibitors of insulin-degrading enzyme with drug-like properties: ebselen (IC_{50} = 14 nM), cefmetazole (IC_{50} = 7 µM) and rabeprazole (IC_{50} = 11 µM). All three compounds are reversible inhibitors of IDE. Docking of cefmetazole and rabeprazole in *h*IDE allowed to rationalize screening results for other compounds in their respective pharmacological class.

Proton-pump inhibitors, have a beneficial impact on the glycemic control of patients with type 2 diabetes, via the possible indirect production of gastrin [48]. Also, this pharmacological class inhibits organic-cation transporters, for which metformin is a substrate, thus impacting metformin pharmacokinetics. Interestingly, though rabeprazole has the same impact on pharmacokinetics of metformin than pantoprazole, it induced a slightly larger decrease in glycemia at 20 mg [49]. Differences of IDE inhibition between rabeprazole and pantoprazole could explain these observations.

Ebselen is the most potent IDE pan-inhibitor described yet (IC_{50} = 14 nM). Unlike rabeprazole and cefmetazole, inhibition of IDE by ebselen is thiol-dependent. HDX-MS and SEC showed that ebselen could impact the dimerization of IDE and that it induces the

disorder of the IDE catalytic cleft significantly differently from **BDM44768** and **6bK**. CETSA on Hep-G2 cells showed IDE-engagement by ebselen in lived cells, illustrating the validation of IDE as a target for this compound. Previously described activities of ebselen in the metabolic field show that ebselen has an insulin-mimetic action. For example, it reduces hyperglycemia induced by diazinon *in vivo* and enhances glucose uptake by peripheral tissues *in vitro* [50]. As well, it restores glucose-stimulated insulin secretion in β-pancreatic cells [51]. Ebselen also controls post-stroke hyperglycemia by improving hepatic insulin signaling and restoring glucose tolerance, in ischemic gerbils [52]. The strong inhibition of IDE by ebselen could participate in these observations. Outside the field of metabolism, a recent clinical trial shows that ebselen is active on the prevention of hearing loss [53]. Ebselen is thought to act by the mimicry and induction of glutathione peroxidase in that context. Interestingly though, one of the substrates of *h*IDE is Insulin-growth factor-I (IGF-I) that is considered as a novel and potent treatment for hear-loss based on various *in vivo* and *in vitro* experiments and clinical trials [54]. As a consequence, ebselen activity in hear-loss could then also be partially mediated by its inhibition of IDE that could increase IGF-I levels.

Altogether, as the inhibitory activity of ebselen towards IDE is the highest listed activity on a human target, we suggest to revisit some of the cellular and *in vivo* effects of ebselen in the light of these results.

4. Experimental section

4.1.1. In vitro IDE activity assays

Wild type human IDE was expressed in *E. coli* BL21 (DE3) cells (at 25 °C and 20 h, 0.5mM IPTG induction using T7 medium) and recombinant IDE were purified by Ni-NTA, source-Q, and three runs of Superdex 200 columns as previously described [10]. Ac-Cys-Lys-Leu-Val-Phe-Phe-Ala-Glu-Asp-Trp-NH_2 was synthesized by NeoMPS. *In vitro* IDE activity was

measured with either a quenched substrate ATTO 655- Cys-Lys-Leu-Val-Phe-Phe-Ala-Glu-Asp-Trp (substrate1) or insulin (Actrapid) from Novo Nordisk. The quantity of insulin was determined using a commercial kit from Perkin Elmer: Human Insulin Kit (catalog#AL204C).

4.1.1.1. *Screening assay*

Human IDE (1.87 ng/µL) was incubated 10 min at 37 °C with compound in Hepes 50 mM, NaCl 100 mM, pH 7.4 and the enzymatic reaction is started by adding the substrate1 (final concentration 5 µM). After 30 min, samples (1% DMSO final) are excited at 635 nm and fluorescence emission at 750 nm is measured on a Victor3 V1420 Perkin Elmer spectrophotometer. EDTA was used as a reference inhibitor (100% inhibition at 2 mM). The Z and Z' factors were calculated according to J.-H. Zhang, T.D.Y. Chung, K.R. Oldenburg, A Simple Statistical Parameter for Use in Evaluation and Validation of High Throughput Screening Assays, J. Biomol. Screen., 4 (1999) 67-73. Data analysis was performed using Xlfit® v 5.0.

4.1.1.2. *Dose-Response Curves*

Percentages of inhibition at different concentrations were obtained as for screening. All measurements were carried out as 8-point dose response curves and reported as the average of at least three independent measurements. EDTA was used as a reference inhibitor (100% inhibition at 2 mM). Data analysis was performed using Xlfit® v 5.0 and GraphPad Prism® v 4.0. Nonlinear curve fitting and statistical analysis was done using built-in functions.

4.1.1.3. *Dose-Response Curves Insulin assay*

400nL of test compounds were added in 96 well microtiter plates (dark, non-binding surface) by acoustic dispensing with Echo (Labcyte), diluted with 9.6 µL of buffer (Hepes at 50 mM with 100 mM NaCl, pH 7,4) and pre-incubated 10 minutes at ambient temperature with 10µL of hIDE wt at 1µg/mL. The enzymatic reaction was started with the addition of 20 µL of insulin at 40 nM for 15 minutes at ambient temperature and stopped with 40 µL of EDTA at

200 mM. Samples were diluted with immunoassay buffer and the content of Insulin was determined by alphaLISA™ according to the manufacturer recommendations. AlphaLISA™ signal is detected with a Mithras (Berthold) using a excitation at 680nm and a emission at 620nm (bandwidth 10nm).

4.1.1.4. *Reversibility.*

Compounds were pre-incubated 30 minutes at room temperature with hIDE before adding substrate (5µM), at final concentrations C and 0.01C respectively as controls. C and 0.01C should surround IC_{50}. C = 1.25 µM for BDM44768 and ebselen, 50 µM for rabeprazole and cefmetazole and 1 mM for N-ethylmaleimide. Pre-incubate at C was diluted 100-fold before adding the substrate. Percents of inhibition are mean of 4 experiments.

4.1.1.5. Analytic size exclusion chromatography

IDE (0.2 mM) in the presence or absence of ebselen (4 mM) were incubated on ice for 1 hr prior to the injection to Superdex S200 column. The molecular weight is estimated based on molecular standard.

4.1.2. Library.

APTEEUS-Université de Lille Library: 1120 compounds including drugs with at least one marketed authorization and active compounds with published record of utilization in humans.

4.1.3. Docking.

Modeling and simulations were performed using 2018.0101 (Chemical Computing Group, Inc.) using non-aged X-ray crystal structure of *h*IDE PDB code 4NXO with BDM44768 ligand. A monomer including solvent was selected and compounds were docked. Before analysis, ligands, solvents and proteins were protonated at 300 °K, pH 7.0 with a salt concentration equal to 0.1 mol/L for the generalized Born / Volume integral (GB/VI) with a

cutoff value of 15. The dielectric constants of solute and solvent are set to 1 and 80, respectively. The method 800R3 was applied to simulate the repulsive part from the van der Waals energy. Then for each compound the industry standard molecular mechanics forcefields MMFF94(s) was used in association with a MOPAC quantum code. The structures were rendered in PyMOL (Delano, W. L. *The PyMOL Molecular Graphics System.* DeLano Scientific LLC: San Carlos, CA, 2002).

4.1.4. Hydrogen-Deuterium Exchange Mass Spectrometry.

HDXMS of IDE in the presence and absence of ebselen was performed similar to the previous reported procedure. Briefly, 14 μM IDE in 8.3 mM Tris-HCl, 50m NaCl, 1.4% DMSO, pH7.2 H_2O buffer was mixed with 140 μM ebselen and incubated at room temperature for 30 min, then kept on ice for 15 min. Functional hydrogen-deuterium exchange reactions were initiated by dilution of 3 μl of stock solution into 9 μl of D_2O buffer (8.3 mM Tris, 50 mM NaCl, pDREAD 7.2) and incubation at 0 °C. The exchange reactions were quenched after various exchange time points (10, 100, 1000, 10000, 100000 sec at 0 °C, and 100000 sec at RT) by adding 18 μl of ice-cold quench buffer containing 0.8% formic acid, 1.6M GuHCl, 16.6% glycerol for a final pH of 2.5. Quenched samples were digested on an immobilized pepsin column (16 μl bed volume). Proteolytic products were collected on a C18 trap column (Michrom Magic C18 AQ 0.2x1 mm) for 1 min desalting and separated using a reverse phase analytical column (Michrom Magic C18 AQ 0.2 x 50 mm, 3 μM) with an acetonitrile linear gradient (6.4%-38.4% over 30min). MS analysis was performed on an OrbiTrap Elite Mass Spectrometer (ThermoFisher Scientific, San Jose, CA). The data was acquired in both data-dependent MS/MS mode and MS1 profile mode and Proteome Discoverer software (ThermoFisher) was used to identify proteolytic peptides. The deuterium content of the peptides for each time point was calculated by DXMS Explorer (Sierra Analytics Inc, Modesto, CA), with corrections for back-exchange [6]. H/D exchange experiments performed

using our automated system typically produce deuteron incorporation measurements with a standard deviation of less than 2% of the mean of triplicate determinations [7-9].

4.1.5. Target engagement by CETSA.

4.1.5.1. Cell culture and drug treatments

HepG2 cells provided by Dr. Nathalie Hennuyer (Pasteur Institute of Lille, France) were cultured in gelatin (Sigma-Aldrich, G-1890, 1 mg/mL) pre coated T75 flasks in MEM Alpha Medium (1X) + GlutaMaxTM (Gibco, 32561-029) containing 10% heat-inactivated fetal calf serum (Life Technologies, 10270-106) and 5µg/mL penicillin/streptomycin (Life Technologies, 15070-063), in 37°C humidified incubator with 5% CO2 atmosphere. Drug treatment was initiated after the cells had grown to confluence with compounds at a final concentration of 30 µM or DMSO for two hours (final vehicle content 0.3%).

4.1.5.2. Whole cell CETSA

Suspension of HepG2 cells were washed in PBS and detached using trypsin/EDTA solution (Life Technologies, 25300054). Cells were transferred in medium in 15 mL Falcon and centrifuged at 300 g during 4 min. Then, the supernatant was discarded and cells were washed in phosphate buffer saline (Gibco, DPBS (1X), 14190-094), counted and centrifuged at 300 g during 4 min. After removing PBS, cells are suspended in Tris Buffered Saline 1X (TBS 10X, Euromedex, ET220-B) at the concentration of 10 million per mL and aliquoted in 10 PCR 0.2 ml microtubes (Thermo Scientific, AB-0622) for each condition with 50 µL. These tubes were then transiently heated to a range of temperature from 40 °C to 67 °C for 3 minutes using a SureCycler 8800 Thermal Cycler (Agilent Technologies), cooled at room temperature for 3 minutes and followed by three freeze/thaw cycles in liquid nitrogen. Insoluble proteins were separated by centrifugation (20000 g, 20 min, 4 °C) and 35 µl of supernatant corresponding to

soluble proteins were kept for Western blot. Three independent experiments were performed for each compound effect characterization.

4.1.5.3. SDS PAGE Electrophoresis with CETSA samples

10 µL of each total protein sample was prepared and heated at 70 °C for 10 min with 1,5 µL of NuPAGE™ Sample Reducing Agent (10X) (Thermoficher Scientific, NP0004) and NuPAGE™ LDS Sample Buffer (4X) (Thermoficher Scientific, NP0007), loaded in NuPage 3-8% Polyacrylamide gel for migration (150V, 1 hour) and then transfer on nitrocellulose membrane (Amersham Protran® supported 0.2 µm NC, 10600080) with iBlot™ 2 Gel Transfer Device (Thermoficher Scientific, IB21001).

4.1.5.4. Immunobloting for Western Blot

Blots and printed membranes were blocked in dry milk (5%) diluted in Phosphate Buffer Saline (PBS) for 1 hour at RT and washed 3 times of 10 min in PBS 0,1% Tween 20. Mouse monoclonal anti-IDE antibody (Santa Cruz Biotechnology, clone F-9, sc-393887) were used as primary antibody diluted at 1:1000 in 2% BSA PBS 0,1% Tween20 solution and incubated 1h30 at RT. After 3 washes in 0,1% PBS Tween 20, Anti-Mouse IRDye 800 CW (Licor IRDye® 800CW Goat anti-Mouse IgG, P/N 925-32210) was used as secondary antibody in 2% BSA PBS 0,1% Tween 20 solution at 1:15000 for 1h30 at RT and blots were washed 3 times of 10 min in PBS Tween 0,1% before fluorescence intensities detection by Odyssey® CLx Imaging System.

4.1.5.5. Data analysis and aggregation curve

Signal intensities (corresponding to Fluorescence minus Background) of each protein band or spot on the Western blots were quantified using Image Studio™ Lite Analysis Software (Licor). For each condition of treatment, fold-changes were calculated in percentage of the

lowest temperature. These relative signals were *plotted* against temperature using Graphpad™ (Prism) and a variable slope sigmoidal curve was fitted using the chemical denaturation theory equation.

$$f(T) = \left(\frac{1 - plateau}{1 + e^{-\left(\frac{a}{T} - b\right)}} \right) + plateau$$

Initial values for top and bottom plateau were set at 100% and 0% respectively for curve fitting. Aggregation curves were expressed as means of multiple experiments (n = 3) +/- SEM. Thermal shifts were calculated using $\Delta T_{Agg}50$, which is the difference in temperatures between the control and treatment, at which 50% signal intensity (protein denaturation) was observed.

4.1.5.6. LC-MS/MS analysis of CETSA samples

To determine the incorporated fraction of compounds in cells for BDM_44768 and ebselen, CETSA samples (10 million cells per ml in TBS) and culture medium containing drugs at 30 µM or vehicle were prepared in a 1 to 20 ratio in an acetonitrile/methanol solution (5:5, v/v). Then, the samples were vigorously mixed with a vortex and centrifuged at 10,000 rpm at 4°C for 10 min, and the supernatants were transferred into tubes for liquid chromatography-mass spectrometry (LC-MS/MS) analysis. Chromatography of 1 µl of the sample was performed on an Acquity BEH C18 column (50*2,1mm 1,7µm, Waters®) by elution with a gradient from Ammonium acetate 10 mM (spontaneous pH) (A) to acetonitrile 0,1 % formic acid (B). The gradient was controlled as follows: 0-0.2 min, 2% B, 0.2-2 min, 2 to 98% B, 2-2.5 min, 98% B, 5.5-2.6 min, 98 to 2% B, 2.6-4 min, 2%B. Flow rate was 0.6 mL/min. Column oven and autosampler temperatures were maintained at 40°C and 10°C respectively. The column outlet of the LC was either connected to Xevo TQD triple Quadrupole Mass Spectrometry (Waters) for MS/MS detection in positive electrospray ionization (ESI) mode. The source temperature was 150 °C, desolvation temperature 600 °C, cone gas flow 50 L/h and desolvation gas flow

1200 L/h. The analytes were monitored in multireaction monitoring mode (MRM). Analyses were processed using MassLynx software (Waters®). The ratio between cellular and medium fraction peak areas permitted to compare the membrane permeability capacities of drugs.

Acknowledgements

The authors acknowledge financial support from INSERM, University of Lille, Institut Pasteur de Lille, Region Nord Pas de Calais, FEDER, Etat (0823007, 0823008, 07-CPER 009-01, 2007-0172-02-CPER/3) , the European Union under the European Regional Fund (ERDF), by the Hauts de France Regional Council (contrat N°17003781), the MEL (contract N°2016_ESR_05), and the French State (contract N°2017-R3-CTRL-Phase 1).and Institut Universitaire de France. P.H. is a recipient of a fellowship from INSERM.

References

[1] K. Yokono, Y. Imamura, K. Shii, H. Sakai, S. Baba, Purification and characterization of insulin-degrading enzyme from pig skeletal muscle, Endocrinology, 108 (1981) 1527-1532.

[2] I.A. Mirsky, R.H. Broh-Kahn, The inactivation of insulin by tissue extracts; the distribution and properties of insulin inactivating extracts. , Archiv. Biochem., 20 (1949) 1-9.

[3] A. Fernandez-Gamba, M.C. Leal, L. Morelli, E.M. Castano, Insulin-degrading enzyme: structure-function relationship and its possible roles in health and disease, Curr. Pharm. Des., 15 (2009) 3644-3655.

[4] W.C. Duckworth, R.G. Bennett, F.G. Hamel, Insulin degradation: progress and potential, Endoc. rev., 19 (1998) 608-624.

[5] W.C. Duckworth, A.E. Kitabchi, Insulin and glucagon degradation by the same enzyme, Diabetes, 23 (1974) 536-543.

[6] R.G. Bennett, W.C. Duckworth, F.G. Hamel, Degradation of amylin by insulin-degrading enzyme, J. Biol. Chem., 275 (2000) 36621-36625.

[7] A.J. Turner, L. Fisk, N.N. Nalivaeva, Targeting amyloid-degrading enzymes as therapeutic strategies in neurodegeneration, Ann. N. Y. Acad. Sci., 1035 (2004) 1-20.

[8] M.A. Leissring, The AβCs of Aβ-cleaving Proteases, J. Biol. Chem., 283 (2008) 29645-29649.

[9] I.V. Kurochkin, Amyloidogenic determinant as a substrate recognition motif of insulin-degrading enzyme, FEBS Lett., 427 (1998) 153-156.

[10] Y. Shen, A. Joachimiak, M.R. Rosner, W.J. Tang, Structures of human insulin-degrading enzyme reveal a new substrate recognition mechanism, Nature, 443 (2006) 870-874.

[11] L.A. McCord, W.G. Liang, E. Dowdell, V. Kalas, R.J. Hoey, A. Koide, S. Koide, W.-J. Tang, Conformational states and recognition of amyloidogenic peptides of human insulin-degrading enzyme, PNAS, 110 (2013) 13827-13832.

[12] Z. Zhang, W.G. Liang, L.J. Bailey, Y.Z. Tan, H. Wei, A. Wang, M. Farcasanu, V.A. Woods, L.A. McCord, D. Lee, W. Shang, R. Deprez-Poulain, B. Deprez, D.R. Liu, A. Koide, S. Koide, A.A. Kossiakoff, S. Li, B. Carragher, C.S. Potter, W.-J. Tang, Ensemble cryoEM elucidates the mechanism of insulin capture and degradation by human insulin degrading enzyme, eLife, 7 (2018) e33572.

[13] G.R. Tundo, D. Sbardella, C. Ciaccio, G. Grasso, M. Gioia, A. Coletta, F. Polticelli, D. Di Pierro, D. Milardi, P. Van Endert, S. Marini, M. Coletta, Multiple functions of insulin-degrading enzyme: a metabolic crosslight?, Crit. Rev. Biochem. Mol. Biol., (2017) 1-29.

[14] M.B. de Tullio, V. Castelletto, I.W. Hamley, P.V. Martino Adami, L. Morelli, E.M. Castano, Proteolytically Inactive Insulin-Degrading Enzyme Inhibits Amyloid Formation Yielding Non-Neurotoxic Aβ Peptide Aggregates, PLoS ONE, 8 (2013) e59113.

[15] D. Sbardella, G.R. Tundo, F. Sciandra, M. Bozzi, M. Gioia, C. Ciaccio, U. Tarantino, A. Brancaccio, M. Coletta, S. Marini, Proteasome Activity Is Affected by Fluctuations in Insulin-Degrading Enzyme Distribution, PLoS One, 10 (2015) e0132455.

[16] M.A. Leissring, E. Malito, S. Hedouin, L. Reinstatler, T. Sahara, S.O. Abdul-Hay, S. Choudhry, G.M. Maharvi, A.H. Fauq, M. Huzarska, P.S. May, S. Choi, T.P. Logan, B.E. Turk, L.C. Cantley, M. Manolopoulou, W.-J. Tang, R.L. Stein, G.D. Cuny, D.J. Selkoe, Designed Inhibitors of Insulin-Degrading Enzyme Regulate the Catabolism and Activity of Insulin, PLoS ONE, 5 (2010) e10504.

[17] J. Charton, M. Gauriot, Q. Guo, N. Hennuyer, X. Marechal, J. Dumont, M. Hamdane, V. Pottiez, V. Landry, O. Sperandio, M. Flipo, L. Buee, B. Staels, F. Leroux, W.-J. Tang, B. Deprez, R. Deprez-Poulain, Imidazole-derived 2-[N-carbamoylmethyl-alkylamino]acetic acids, substrate-dependent modulators of insulin-degrading enzyme in amyloid-β hydrolysis, European Journal of Medicinal Chemistry, 79 (2014) 184-193.

[18] J. Charton, M. Gauriot, J. Totobenazara, N. Hennuyer, J. Dumont, D. Bosc, X. Marechal, J. Elbakali, A. Herledan, X. Wen, C. Ronco, H. Gras-Masse, A. Heninot, V. Pottiez, V. Landry, B. Staels, W.G. Liang, F. Leroux, W.J. Tang, B. Deprez, R. Deprez-Poulain, Structure-activity relationships of Imidazole-derived 2-[N-carbamoylmethyl-alkylamino]acetic acids, dual binders of human Insulin-Degrading Enzyme, Eur J Med Chem, 90 (2015) 547-567.

[19] J.P. Maianti, A. McFedries, Z.H. Foda, R.E. Kleiner, X.Q. Du, M.A. Leissring, W.-J. Tang, M.J. Charron, M.A. Seeliger, A. Saghatelian, D.R. Liu, Anti-diabetic activity of insulin-degrading enzyme inhibitors mediated by multiple hormones, Nature, 511 (2014) 94-98.

[20] T.B. Durham, J.L. Toth, V.J. Klimkowski, J.X.C. Cao, A.M. Siesky, J. Alexander-Chacko, G.Y. Wu, J.T. Dixon, J.E. McGee, Y. Wang, S.Y. Guo, R.N. Cavitt, J. Schindler, S.J.

Thibodeaux, N.A. Calvert, M.J. Coghlan, D.K. Sindelar, M. Christe, V.V. Kiselyov, M.D. Michael, K.W. Sloop, Dual Exosite-binding Inhibitors of Insulin-degrading Enzyme Challenge Its Role as the Primary Mediator of Insulin Clearance in Vivo, Journal of Biological Chemistry, 290 (2015) 20044-20059.

[21] R. Deprez-Poulain, N. Hennuyer, D. Bosc, W.G. Liang, E. Enée, X. Marechal, J. Charton, J. Totobenazara, G. Berte, J. Jahklal, T. Verdelet, J. Dumont, S. Dassonneville, E. Woitrain, M. Gauriot, C. Paquet, I. Duplan, P. Hermant, F.-X. Cantrelle, E. Sevin, M. Culot, V. Landry, A. Herledan, C. Piveteau, G. Lippens, F. Leroux, W.-J. Tang, P. van Endert, B. Staels, B. Deprez, Catalytic site inhibition of insulin-degrading enzyme by a small molecule induces glucose intolerance in mice, Nat. Commun., 6 (2015) 8250.

[22] P. Mishra, A.N. Dauphinee, C. Ward, S. Sarkar, A.H.L.A.N. Gunawardena, R. Manjithaya, Discovery of pan autophagy inhibitors through a high-throughput screen highlights macroautophagy as an evolutionarily conserved process across 3 eukaryotic kingdoms, Autophagy, (2017) 1-17.

[23] S.J. Gosai, J.H. Kwak, C.J. Luke, O.S. Long, D.E. King, K.J. Kovatch, P.A. Johnston, T.Y. Shun, J.S. Lazo, D.H. Perlmutter, G.A. Silverman, S.C. Pak, Automated high-content live animal drug screening using C. elegans expressing the aggregation prone serpin alpha1-antitrypsin Z, PLoS One, 5 (2010) e15460.

[24] Y.T. Ghebremariam, P. LePendu, J.C. Lee, D.A. Erlanson, A. Slaviero, N.H. Shah, J. Leiper, J.P. Cooke, Unexpected Effect of Proton Pump Inhibitors, Circulation, 128 (2013) 845.

[25] Y. Bi, M. Might, H. Vankayalapati, B. Kuberan, Repurposing of Proton Pump Inhibitors as first identified small molecule inhibitors of endo-beta-N-acetylglucosaminidase (ENGase) for the treatment of NGLY1 deficiency, a rare genetic disease, Bioorg. Med. Chem. Lett., 27 (2017) 2962-2966.

[26] T. Nikawa, G. Schuch, G. Wagner, H. Sies, Interaction of ebselen with glutathione S-transferase and papain in vitro, Biochem. Pharmacol., 47 (1994) 1007-1012.

[27] R. Zhao, H. Masayasu, A. Holmgren, Ebselen: a substrate for human thioredoxin reductase strongly stimulating its hydroperoxide reductase activity and a superfast thioredoxin oxidant, Proc. Natl. Acad. Sci. U. S. A., 99 (2002) 8579-8584.

[28] G.K. Azad, R.S. Tomar, Ebselen, a promising antioxidant drug: mechanisms of action and targets of biological pathways, Mol. Biol. Rep., 41 (2014) 4865-4879.

[29] T. Schewe, Molecular actions of Ebselen—an antiinflammatory antioxidant, General Pharmacology: The Vascular System, 26 (1995) 1153-1169.

[30] C. Schewe, T. Schewe, A. Wendel, Strong inhibition of mammalian lipoxygenases by the antiinflammatory seleno-organic compound ebselen in the absence of glutathione, Biochem. Pharmacol., 48 (1994) 65-74.

[31] T. Takasago, E.E. Peters, D.I. Graham, H. Masayasu, I.M. Macrae, Neuroprotective efficacy of ebselen, an anti-oxidant with anti-inflammatory actions, in a rodent model of permanent middle cerebral artery occlusion, Br. J. Pharmacol., 122 (1997) 1251-1256.

[32] T. Yamaguchi, K. Sano, K. Takakura, I. Saito, Y. Shinohara, T. Asano, H. Yasuhara, Ebselen in Acute Ischemic Stroke, Stroke, 29 (1998) 12-17.

[33] E.S. Inks, B.J. Josey, S.R. Jesinkey, C.J. Chou, A Novel Class of Small Molecule Inhibitors of HDAC6, ACS Chem. Biol., 7 (2012) 331-339.

[34] E. Węglarz-Tomczak, M. Burda-Grabowska, M. Giurg, A. Mucha, Identification of methionine aminopeptidase 2 as a molecular target of the organoselenium drug ebselen and its derivatives/analogues: Synthesis, inhibitory activity and molecular modeling study, Bioorg. Med. Chem. Lett., 26 (2016) 5254-5259.

[35] Y. Yu, Y. Jin, J. Zhou, H. Ruan, H. Zhao, S. Lu, Y. Zhang, D. Li, X. Ji, B.H. Ruan, Ebselen: Mechanisms of Glutamate Dehydrogenase and Glutaminase Enzyme Inhibition, ACS Chem. Biol., 12 (2017) 3003-3011.

[36] J. Chiou, S. Wan, K.-F. Chan, P.-K. So, D. He, E.W.-c. Chan, T.-h. Chan, K.-y. Wong, J. Tao, S. Chen, Ebselen as a potent covalent inhibitor of New Delhi metallo-[small beta]-lactamase (NDM-1), Chem. Commun., 51 (2015) 9543-9546.

[37] S. Thangamani, W. Younis, M.N. Seleem, Repurposing ebselen for treatment of multidrug-resistant staphylococcal infections, 5 (2015) 11596.

[38] C.M. Goins, S. Dajnowicz, S. Thanna, S.J. Sucheck, J.M. Parks, D.R. Ronning, Exploring Covalent Allosteric Inhibition of Antigen 85C from Mycobacterium tuberculosis by Ebselen Derivatives, ACS Infectious Diseases, 3 (2017) 378-387.

[39] H.M. Gordhan, S.L. Patrick, M.I. Swasy, A.L. Hackler, M. Anayee, J.E. Golden, J.C. Morris, D.C. Whitehead, Evaluation of substituted ebselen derivatives as potential trypanocidal agents, Bioorg. Med. Chem. Lett., 27 (2017) 537-541.

[40] S. Thenin-Houssier, I.M.S. de Vera, L. Pedro-Rosa, A. Brady, A. Richard, B. Konnick, S. Opp, C. Buffone, J. Fuhrmann, S. Kota, B. Billack, M. Pietka-Ottlik, T. Tellinghuisen, H. Choe, T. Spicer, L. Scampavia, F. Diaz-Griffero, D.J. Kojetin, S.T. Valente, Ebselen, a Small-Molecule Capsid Inhibitor of HIV-1 Replication, Antimicrob. Agents Chemother., 60 (2016) 2195-2208.

[41] S. Mukherjee, W.S. Weiner, C.E. Schroeder, D.S. Simpson, A.M. Hanson, N.L. Sweeney, R.K. Marvin, J. Ndjomou, R. Kolli, D. Isailovic, F.J. Schoenen, D.N. Frick, Ebselen inhibits hepatitis C virus NS3 helicase binding to nucleic acid and prevents viral replication, ACS Chem. Biol., 9 (2014) 2393-2403.

[42] A.E.Y. Sarwono, S. Mitsuhashi, M.H.B. Kabir, K. Shigetomi, T. Okada, F. Ohsaka, S. Otsuguro, K. Maenaka, M. Igarashi, K. Kato, M. Ubukata, Repurposing existing drugs:

identification of irreversible IMPDH inhibitors by high-throughput screening, J. Enzyme Inhib. Med. Chem., 34 (2019) 171-178.

[43] E.S. Song, M. Melikishvili, M.G. Fried, M.A. Juliano, L. Juliano, D.W. Rodgers, L.B. Hersh, Cysteine 904 is required for maximal insulin degrading enzyme activity and polyanion activation, PLoS One, 7 (2012) e46790.

[44] M. Manolopoulou, Q. Guo, E. Malito, A.B. Schilling, W.J. Tang, Molecular basis of catalytic chamber-assisted unfolding and cleavage of human insulin by human insulin-degrading enzyme, J. Biol. Chem., 284 (2009) 14177-14188.

[45] Z. Chen, Z. Jiang, N. Chen, Q. Shi, L. Tong, F. Kong, X. Cheng, H. Chen, C. Wang, B. Tang, Target discovery of ebselen with a biotinylated probe, Chem. Commun., 54 (2018) 9506-9509.

[46] E.S. Song, D.W. Rodgers, L.B. Hersh, Insulin-degrading enzyme is not secreted from cultured cells, Scientific Reports, 8 (2018) Article number: 2335.

[47] K.M. Comess, S.M. McLoughlin, J.A. Oyer, P.L. Richardson, H. Stöckmann, A. Vasudevan, S.E. Warder, Emerging Approaches for the Identification of Protein Targets of Small Molecules - A Practitioners' Perspective, J. Med. Chem., 61 (2018) 8504-8535.

[48] K. Takebayashi, T. Inukai, Effect of proton pump inhibitors on glycemic control in patients with diabetes, World journal of diabetes, 6 (2015) 1122-1131.

[49] A. Kim, I. Chung, S.H. Yoon, K.S. Yu, K.S. Lim, J.Y. Cho, H. Lee, I.J. Jang, J.Y. Chung, Effects of proton pump inhibitors on metformin pharmacokinetics and pharmacodynamics, Drug Metab. Dispos., 42 (2014) 1174-1179.

[50] M.D. Costa, B.M. Gai, C.I. Acker, A.C. Souza, R. Brandao, C.W. Nogueira, Ebselen reduces hyperglycemia temporarily-induced by diazinon: a compound with insulin-mimetic properties, Chem. Biol. Interact., 197 (2012) 80-86.

[51] X. Wang, J.-W. Yun, X.G. Lei, Glutathione Peroxidase Mimic Ebselen Improves Glucose-Stimulated Insulin Secretion in Murine Islets, Antioxidants & Redox Signaling, 20 (2014) 191-203.

[52] S. Park, S. Kang, D.S. Kim, B.K. Shin, N.R. Moon, J.W. Daily, Ebselen pretreatment attenuates ischemia/reperfusion injury and prevents hyperglycemia by improving hepatic insulin signaling and β-cell survival in gerbils, Free Radic. Res., 48 (2014) 864-874.

[53] J. Kil, E. Lobarinas, C. Spankovich, S.K. Griffiths, P.J. Antonelli, E.D. Lynch, C.G. Le Prell, Safety and efficacy of ebselen for the prevention of noise-induced hearing loss: a randomised, double-blind, placebo-controlled, phase 2 trial, Lancet, 390 (2017) 969-979.

[54] K. Yamahara, N. Asaka, T. Kita, I. Kishimoto, M. Matsunaga, N. Yamamoto, K. Omori, T. Nakagawa, Insulin-like growth factor 1 promotes cochlear synapse regeneration after excitotoxic trauma in vitro, Hear. Res., 374 (2019) 5-12.